Chapter 2.   Semiconductor Surface Studies

Academic and Research Staff

Professor John D. Joannopoulos, Dr. Kyeongjae Cho, Dr. Susanne Mirbt, Dr. Pierre R. Villeneuve

Graduate Students

Shanhui Fan, Attila Mekis, Ickjin Park, Tairan Wang

Technical and Support Staff

Margaret E. O'Meara

2.1   Introduction

Sponsor

Understanding the properties of surfaces of solids and the interactions of atoms and molecules with surfaces has been of extreme importance from both technological and academic points of view. The advent of ultrahigh vacuum technology has made microscopic studies of well-characterized surface systems possible. The way atoms move to reduce the energy of their surface, the number of layers of atoms involved in this reduction, the electronic and vibrational states that result from this movement, and the final symmetry of the surface layer are all of utmost importance in arriving at a fundamental and microscopic understanding of the nature of clean surfaces, chemisorption processes, and the initial stages of interface formation.

The theoretical problems associated with these systems are quite complex. However, we are currently at the forefront of solving the properties of real surface systems. In particular, we are continuing our efforts in developing new techniques for calculating the total ground-state energy of a surface system from "first principles" so that we can provide accurate theoretical predictions of surface geometries and behavior. Our efforts in this program have been concentrated in the areas of surface defects, surface reconstruction geometries, structural phase transitions, and novel computational techniques.

2.2   Adatom Vacancies on the Si(111)– (7x7) Surface

The Si(111) surface is the natural cleavage surface for silicon crystals and the structure of the (111) surface reconstruction has been extensively studied both experimentally and theoretically. More than 35 years have passed since the first identification by low-energy electron diffraction (LEED) of the (7x7) symmetry after annealing of the (111) surface. Understanding the structure of this large reconstruction unit has been one of the most outstanding surface problems since then. Currently, the Takayanagi dimer-adatom-stacking-fault (DAS) structure is generally accepted as the correct model for the structure of the (7x7) reconstruction.

Because of the complexity of the (7x7) reconstruction, first-principles theoretical investigations of the (111) surface have been a challenging task. Almost as important as the determination of the equilibrium structure, however, is the understanding of the microscopic dynamical processes in the phase transition of the surface reconstruction from the (7x7) symmetry to the (1x1) at around 870°C. The (7x7) reconstruction rearranges the three topmost surface layer atoms from the bulk-truncated surface, and one can easily imagine the complexity of the rearrangement process from the number of rearranged atoms in each (7x7) unit (i.e., 102 atoms). Among these three layers, the top surface layer consists of adatoms, and each adatom is expected to be weakly bound to the surface atoms' four strained backbonds. Because of this weak binding, removal of the adatom layer will naturally initiate the complicated dynamical processes of the surface phase transition.

In this work, we investigate the formation of adatom vacancies using total-energy pseudopotential calculations. The average adatom vacancy formation energy is found to be 0.9 eV, with small (~0.1 eV) variations for the four types of surface adatoms. These results are in marked contrast to experimental estimates which lie around 0.4 eV. We also predict changes in the electronic structure of surface states induced by local modifications in geometry at the

vicinity of the vacancy. These changes should be readily observable in differential scanning tunneling microscopy (STM).

Our calculated adatom vacancy formation energies are listed in Table 1. Our results predict adatom removal energies of 0.9 eV on average. We note that these energies are smaller than surface atom vacancy formation energies calculated for the (2x1) reconstruction which are around 2.3 eV. The differences in vacancy formation energies among the adatoms, albeit small (typically 0.1 eV), reveal a distinct pattern: it is easier to remove a corner adatom than an edge adatom on the same side (faulted or unfaulted) of the unit cell, and it is also easier to remove an adatom on the faulted side than a corresponding one (edge or corner) on the unfaulted side. The interplay between geometry and strain considerations provides a physical explanation for these differences. First, the resulting stress introduced by removing an adatom from a corner site is more effectively dissipated due to the "extra" surface area in the vicinity of the corner hole, leading to a smaller removal energy for corner adatoms. Second, notice that the difference between faulted and unfaulted halves is only revealed by the tight-binding relaxation of the bulk layers (fourth layer and below). The explanation for this difference is subtle and requires a careful analysis of the strain fields associated with the (7x7) structure.

Table 1: **Vacancy formation energies (in eV) of four types of adatoms (1-4 as idicated in Figure 1). The tight-binding (TB) correction is the energy difference between the four-layer lab calculations.**

	ab initio	TB correction	Formation energy
Unfaulted corner (1)	0.88	0.03	0.91
Unfaulted edge (2)	1.00	0.02	1.02
Faulted corner (3)	0.94	-0.13	0.81
Faulted edge (4)	0.99	-0.11	0.88

Our results show important discrepancies when compared to available experimental results. Experimental measurements of adatom vacancy formation energies constitute a difficult task. A first attempt was made by Uchida et al.[1] In their work, site-specific field evaporation of adatoms was performed, and variations in adatom removal probabilities for each site were interpreted as arising directly from differences in adatom binding energies. Their results suggest a very small (0.01 eV) difference in binding energy between corner and edge adatoms. No measurable difference was observed between faulted and unfaulted adatom binding energies. However, the interpretation of field evaporation experiments can be extremely nontrivial, especially because the adatoms have to be ionized before being removed. Local softness analysis shows that each adatom has a different chemical reactivity leading to a different ionization energy. Besides, atoms can ionize into several charge states, corresponding to different channels in the evaporation process and making the analysis of the results very complicated.

A more direct approach was taken by Tsong et al.[2] They performed a high-temperature (840°C) anneal of the (7x7) surface, followed by a rapid quench and subsequent analysis of the vacancy concentration by STM. By assuming thermodynamic equilibrium at the annealing temperture, vacancy formation energies were determined to be 0.476 eV, 0.361 eV, 0.463 eV and 0.360 eV for unfaulted corner, unfaulted edge, faulted corner, and faulted edge adatoms, respectively. However, at such a high temperature [close to the (7x7)-to-(1x1) phase transition temperature], the adatoms are very mobile and are expected to form a "fluid" phase. This kind of behavior would affect completely the measured vacancy formation energy.

1   H. Uchida, D. Huang, F. Grey, and M. Aono, *Phys. Rev. Lett.* 70: 2040 (1993).

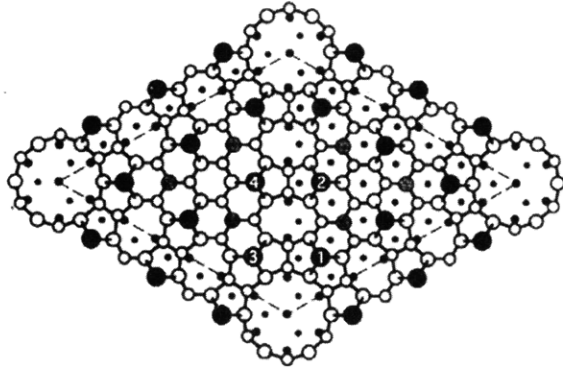2   T.T. Tsong, R.-L. Lo, T.-C. Chang, and C. Chen, *Surf. Rev. Lett.* 1: 197 (1994).

Notice also that the vacancy dangling bonds look dimmer when compared to the rest atom dangling bonds.

An estimate of the total charge on these localized orbitals reveals that each vacancy dangling bond contains about two-thirds of the electronic charge of the rest atom dangling bonds. An analogous situation can be seen for the unfaulted edge adatom removal in Figure 4. Again, the three vacancy dangling bonds lie at higher energy than the other rest atom dangling bonds. Positive bias calculations reveal the same qualitative behavior but the images are not as striking because the empty states close to the Fermi level do not have much of a contribution from the dangling bonds of interest.
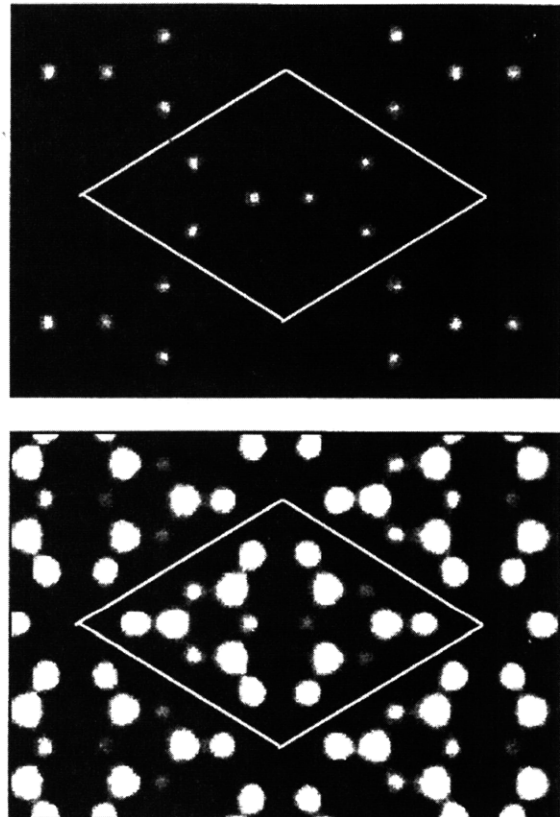

Figure 1. Top view of the (7X7) DAS reconstruction. The four nonequivalent types of adatoms are labeled unfaulted corner (1), unfaulted edge (2), faulted corner (3), and faulted edge (4).

Let us now focus our attention on the changes introduced in the electronic structure by removal of an adatom. Particularly, we are interested in dangling-bond states, not only because of their importance as far as surface reactivity is concerned, but also because they are more easily observed in STM experiments. Details in the surface electronic structure are best described in differential STM images, which allow an energy-resolved analysis of the electronic states. To our knowledge, this type of measurement has not yet been used to study vacancies in the (7X7) surface.

Figure 2 shows theoretical differential "constant-height" STM images for the perfect surface at different energy ranges, 0 to 0.2 eV and 0.2 to 0.5 eV from the Fermi level. Notice that for energies closer to the Fermi level, only the adatom dangling bonds appear in the image (primarily on the edge adatoms), whereas for lower energies, contributions from the rest atoms are also evident. Let us now describe how this picture changes when an adatom is removed from the surface.

We will focus our analysis on the unfaulted side of the unit cell; the faulted side behaves similarly in this aspect. Consider first an unfaulted corner adatom being removed (labeled 1 in Figure 1). STM images corresponding to the same energy ranges as Figure 3 are displayed in Figure 2 for this case. Notice that besides the adatom dangling bonds, the three newly formed vacancy dangling bonds and the rest atom dangling bond closest to them can also be observed within 0.2 eV of the Fermi level. The other five rest atom dangling bonds remain at lower energies.

Figure 2. Constant-height STM simulation for the perfect surface. Top panel, from 0.0 eV to −0.2 eV; notice the adatom dangling bonds. Bottom panel, from −0.2 eV to −0.5 eV; rest atom and adatom dangling bonds. The height is 2 Å above the adatom layer, and the white lines mark the unit cell boundaries in all STM plots.

These changes in electronic structure can be understood by simple consideration of orbital character and structural relaxations. To first approximation, we would expect that all rest atom and vacancy dangling bonds lie in the same energy range, since they are very similar in terms of local geometry. This is not completely true, however, because of the "popped-up" nature of the rest atoms. Rest atoms are subject to a stress due to the presence of adatoms, which makes their backbonds have angles that are considerably smaller than the tetrahedral angle, thus giving more s character to the dangling-bond state and lowering its energy. Once a vacany is formed, however, the stress is locally reduced for the rest atom(s) closest to the vacancy (two for an edge vacancy and one for a corner vacancy). Therefore, the angles betweenbackbonds increase, making these dangling-bond states more p-like in character and thus raising their energy. The angles between backbonds of the "vacancy atoms" are also large, so that the vacancy dangling bonds lie close in energy to the relaxed atoms (within 0.2 eV of the Fermi energy).
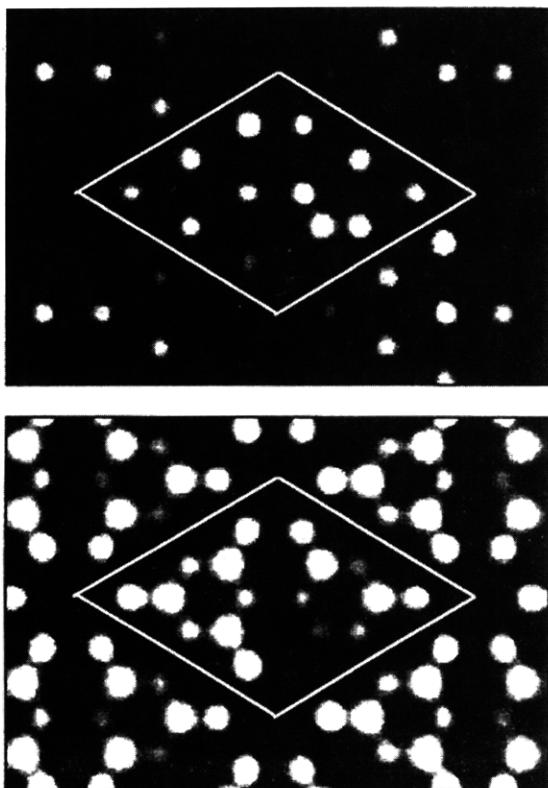

Figure 3. Constant-height STM simulation for vacancy 1. Top panel, from 0.0 eV to –0.2 eV; besides the adatoms notice also the three vacancy dangling bonds and the rest atom dangling bond closest to them. Bottom panel, from –0.2 eV to –0.5 eV; the remaining rest atom and adatom dangling bonds.
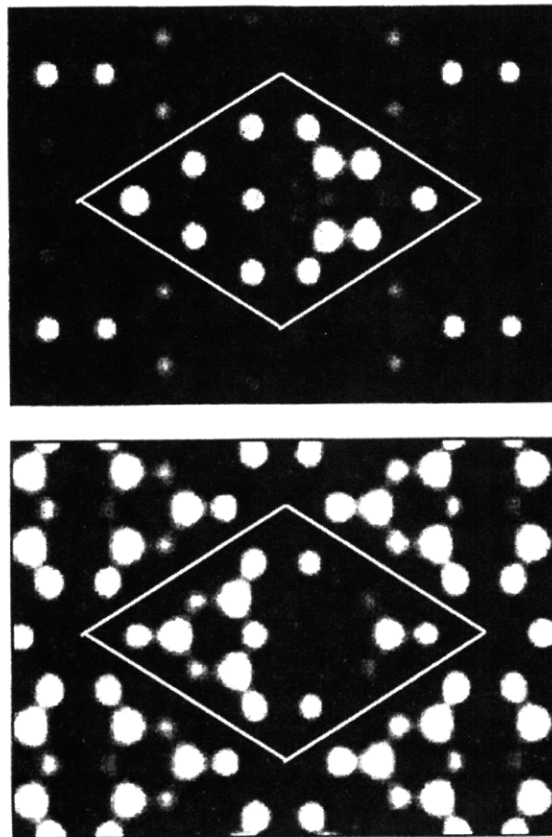

Figure 4. Constant-height STM simulation for vacancy 2. Top panel, from 0.0 eV to –0.2 eV; besides the adatoms notice also the three vacancy dangling bonds and the two rest atom dangling bonds closest to them. Bottom panel, from –0.2 eV to –0.5 eV; the remaining rest-atom and adatom dangling bonds.

2.3 Unified Approach for Calculation of Force-Constants and Accelerated Convergence of Atomic Coordinates

The search for increasingly efficient ways to obtain the atomic and electronic coordinates which minimize the total energy of a given system has been one of the greatest challenges in computational condensed matter physics in the past few years. Most recent developments in the field have focused on the treatment of the formidable electronic problem. Therefore the conceptually more simple relaxation of atomic coordinates (which in most cases can be treated classically) has been somewhat overlooked. But, with the realm of *ab initio* calculations approaching systems with thousands of atoms and beyond,

atomic relaxations will have to be performed under increasingly stricter tolerances in order to preserve the accuracy of total energy calculations.

Atomic relaxations can be performed merely by moving the atoms in the direction of their Hellman-Feynman forces by an amount which is determined by an effective force constant of the system. Despite wide use because of its simplicity, this "steepest descent" procedure is clearly not the most efficient manner to perform atomic relaxations for large, inhomogeneous systems. In addition, the route towards the ground state contains a huge amount of information about the lattice dynamics of the system which is often completely ignored. When compared to ground-state properties, *ab initio* calculations of dynamical properties (i.e., vibrational frequencies and normal modes) are still in their early stage, as far as system sizes are concerned. New developments which could bring together the frontiers of ground-state and dynamical *ab initio* calculations would be very desirable.

In this work, we propose a simple and efficient procedure to perform atomic relaxations which provides the force constant matrix (FCM) of the system *with no additional cost*. Instead of applying perturbations to the equilibrium configuration, the FCM is optimized *as we move the atoms towards the ground state* and simultaneously used to calculate atomic displacements which will further relax the atoms. As we shall see below, the method provides, in a unified way, largely accelerated convergence to the equilibrium atomic positions and a good description of the dynamical properties.

The FCM, ϕ, is defined through its matrix elements ϕ_{ij} in the usual way:

$$\Phi_{ij} = \left.\frac{\partial^2 E}{\partial R_i R_j}\right|_{R_0} , \qquad (1)$$

where E is the total energy and R is a 3N-component vector describing the atomic positions. The derivatives are evaluated at the ground-state configuration. Assuming small displacements from equilibrium $u = R - R_0$ such that the harmonic approximation is valid, one can calculate the atomic forces as $F = -\Phi \cdot u$ or, equivalently, obtain the displacements u (and therefore the ground-state configuration) from given forces and the inverse force constant matrix Φ^{-1}.

However, the FCM of a generic system is not known, and most existing methods for calculating it are based on applying perturbations to a system where

the ground-state configuration *is already known*. For instance, in a "finite-difference" approach, if a small displacement is applied to an atom and the force on another atom is calculated, the corresponding matrix element of Φ would be simply minus the ratio between force and displacement. Inspired by this procedure, one could use the atomic displacements that are naturally produced in the relaxation process and combine them with the corresponding variations in atomic forces in order to obtain increasingly better approximations to the FCM.

In the lth ionic iteration, defined by the change in atomic positions $\Delta R^{(l)}$, there is a corresponding variation in the forces, $\Delta F^{(l)}$. In the harmonic regime these two quantities are related by

$$(\Delta F^{(l)} = -\Phi \cdot \Delta R^{(l)}) \quad . \qquad (2)$$

Our task is then to find the optimum Φ which relates the two known variations $\Delta R^{(l)}$ and $\Delta F^{(l)}$. However, equation (2) imposes only 3N constraints on Φ, so an impractical number of ionic iterations would be required in order to uniquely determine all the $(3N)^2$ elements of the FCM. Nevertheless, one can progressively improve an initial guess Φ_0 by minimizing the quantity

$$\varepsilon = \sum_l \omega_l^2 \left|\Phi \cdot \Delta R^{(l)} + \Delta F^{(l)}\right|^2 + \omega'^2 \left\|(\Phi - \Phi_0)\right\|^2 , \qquad (3)$$

where the sum over l runs over all previous iterations and the weights ω_l and ω' are added to provide more flexibility to the method. This is the essence of the modified Broyden scheme.

For systems complicated enough so that a good initial guess Φ_0 is not known, the FCM in the modified Broyden method is expected to converge very slowly to the true Φ. This can be seen as an intrinsic limitation of the method in trying to obtain simultaneously the $(3N)^2$ elements of Φ from a limited amount of information provided by the set of equations (2).

One can overcome these limitations by realizing that not all the matrix elements of Φ are independent and, more importantly, they are not equally relevant. Therefore we can reduce substantially the number of free parameters to be determined by including all the symmetry information of our system in the FCM, and by imposing a sensible cutoff in the matrix elements, beyond which they are either set to zero or described by an approximate model. With this goal in mind, we define a "parameter vector" p with N_p coordinates,

where the number of parameters (N_p) is now much smaller than $(3N)^2$. The matrix elements of Φ are then expanded in these N_p parameters:

$$\Phi_{ij} = \sum_{k=1}^{N_p} \alpha_{ijk} p_k \quad , \tag{4}$$

where α_{ijk} is a ($3N \times 3N \times N_p$) tensor which contains all information about symmetry and cutoff distance of the FCM. The quantity to be minimized now is simply

$$\varepsilon = \sum_l \omega_l^2 \left| \Phi \cdot \Delta R^{(l)} + \Delta F^{(l)} \right|^2 \quad . \tag{5}$$

Notice that an initial guess for Φ is not necessary anymore, since the number of parameters N_p can always be chosen to be smaller than $3N$ times the number of previous iterations. Now, setting $\partial\varepsilon / p_k = 0$ gives the simple formula:

$$p = -\mu^{-1} \cdot v \quad . \tag{6}$$

where

$$\mu = \sum_l \omega_l^2 A^{(l)^T} \cdot A^{(l)} \quad , \tag{7}$$

$$v = \sum_l \omega_l^2 A^{(l)^T} \cdot \Delta F^{(l)} \quad , \tag{8}$$

and the $A^{(l)}$'s are ($3N \times N_p$) matrices defined by

$$A_{ik}^{(l)} = \sum_j \alpha_{ijk} \Delta R_j^{(l)} \quad . \tag{9}$$

The parametrized FCM is then inverted, and displacements from equilibrium are calculated and used to move the atoms. This process is repeated until convergence is achieved.

We now test the effectiveness of this procedure in describing relaxations to the ground state in bulk silicon. Local-density-functional pseudopotential total-energy calculations are performed on a cubic 64-atom unit cell with Γ-point sampling and a plane-wave energy cutoff of 8 Ry. The atoms are initially displaced at random from their equilibrium positions, by an amount defined by a random value between –0.2 and 0.2 Å for each Cartesian direction.

In Figure 5, we compare the performance of our parametrized FCM method with the modified Broyden method and the steepest descent method as we relax the system towards the ground state. The improvement obtained by using our FCM with just a few parameters is evident. Energy convergence within 10^{-5} eV is obtained in just seven iterations, whereas at least 46 steepest descent moves or 19 modified Broyden moves would be required in order to reach the same convergence level. The reason for this improvement in convergence is related to the fact that the parametrized FCM approach provides a much better approximation to the true force constant matrix in just a few iterations.
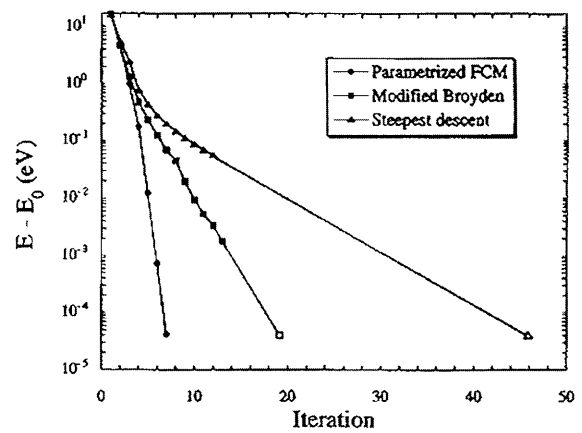

Figure 5. Energy convergence as a function of the num-ber of iterations for the steepest descent, modified Broyden and parametrized FCM methods. An effective force constant of 20 eV/Å² was used for the steepest descent moves. The Φ_0 in the modified Broyden scheme was initialized to be a constant-diagonal matrix with magnitude 20 eV/Å². The empty square and triangle are linear extrapolations of the modified Broyden and steepest descent results, respectively.

We are now in position to obtain the phonon spectrum of bulk silicon by diagonalizing the dynamical matrix. Our results are displayed in Figure 6, where we compare our calculated phonon frequencies to an independent determination using *ab initio* molecular dynamics in the same unit cell and with identical conditions of plane wave cutoff and k-point sampling. Comparison between these two calculations directly probes the consequences of imposing a cutoff in Φ, and it is clear that this approach works extremely well. Also, in the same figure, we plot the experimental vibrational frequencies. Our calculated frequencies deviate 2.6% on average from the experimental ones, the largest deviation being on the TO mode and the X point (8.6%). Notice that the flat TA modes

are described beautifully. This demonstrates that our method can produce accurate vibrational frequencies with no fitting parameters. A more elaborate description of the long-range forces could be used if one needs to improve even more on this agreement.
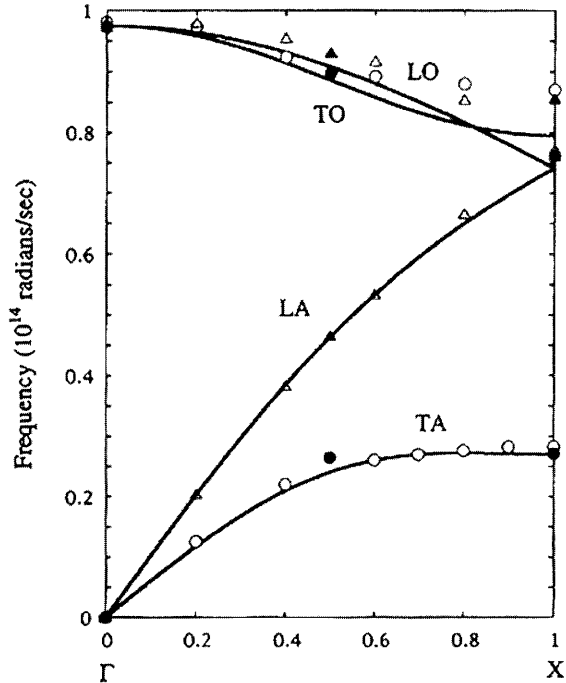

Figure 6. Calculated (lines and filled dots) and experimental (open dots) phonon frequencies along Γ- X triangles for longitudinal modes and circles for transverse modes.

2.4 Publications

Aydinol, M., A. Kohan, G. Ceder, K. Cho, and J. Joannopoulos. "Ab-initio Study of Li Intercalation in Metal Oxides and Metal Dichalcogenides." *Phys. Rev. B* 56: 1354 (1997).

Chen, J., S. Fan, A. Mekis, I. Kurland, P. Villeneuve, K. Li, H. Haus, and J. Joannopoulos. "Finite Differencing of Periodic Structures." *SPIE Proc.* 2994: (1997).

Cho, K., E. Kaxiras, and J. Joannopoulos. "Theory of Adsorptiona and Desorption of H2 Molecules on the Si(111)–(7X7) Surface." *Phys. Rev. Lett.,* Forthcoming.

Fan, S., P. Villeneuve, J. Joannopoulos, and F. Schubert. "Photonic Crystal LED's." *SPIE Proc.* 3002: 67 (1997).

Fan, S., P. Villeneuve, J. Joannopoulos, and F. Schubert. "High Extraction Efficiency of Spontaneous Emission from Slabs of Photonic Crystals." *Phys. Rev. Lett.* 78: 3294 (1997).

Fan, S., P. Villeneuve, J. Joannopoulos, and H. Haus. "Channel Drop Tunneling through Localized States." *Phys. Rev. Lett.* Forthcoming.

Foresi, J., P. Villeneuve, J. Ferrara, E. Thoen, G. Steinmeyer, S. Fan, J. Joannopoulos, L. Kimerling, H. Smith, and E. Ippen. "Photonic Bandgap Microcavities in Optical Waveguides." *Nature* 390: 143 (1997).

Joannopoulos, J.D., P. Villeneuve, and S. Fan. "Photonic Crystals." *Solid State Commun.* 102: 165 (1997).

Joannopoulos, J., P. Villeneuve, and S. Fan. "Photonic Crystals: Putting a New Twist on Light." *Nature* 386: 143 (1997).

Villeneuve, P., S. Fan, A. Mekis, and J. Joannopoulos. "Photonic Crystals and Their Potential Applications." *Proc. IEE* England (1997).